Extended Abstracts of the 2018 International Conference on Solid State Devices and Materials, Tokyo, 2018, pp1043-1044

Fabrication of $CH_3NH_3PbI_3/CH_3NH_3PbCl_3$ Heterostructure using Vacuum Evaporation

Tomonori Matsushita, Shun Takashima, Yuiga Nakamura and Takashi Kondo

The University of Tokyo
4-6-1, Komaba, Meguro-ku
Tokyo 153-8904, Japan
Phone: +81-3-5841-5170, E-mail: mtomo@castle.t.u-tokyo.ac.jp

Abstract

We have successfully fabricated single- and double-heterostructures of lead halide perovskites using sequential vacuum evaporation. Combination of $CH_3NH_3PbI_3$ and $CH_3NH_3PbCl_3$ leads to formation of heterostructures presumably because of considerably suppressed interdiffusion of iodide and chloride ions caused by large mismatch of ion radii.

1. Introduction

Lead halide perovskite semiconductors are promising materials not only for high-efficiency solar cells but also for light emitting and photodetection devices. The heterostructure fabrication of the perovskite semiconductors would further expand the possibility of perovskite applications and enables us to realize all perovskite devices and quantum-well based photonic devices. However, fabrication of lead halide perovskite heterostructures has not been successful to date. $CH_3NH_3PbI_3$ and $CH_3NH_3PbBr_3$ layers stacked by using pulsed laser deposition or vacuum deposition were found to be spontaneously alloyed [1, 2], and single $CH_3NH_3Pb(I_{1-x}Br_x)_3$ layers were formed because of interdiffusion of halide ions via halogen vacancies [3]. On the other hand, it is reported that $CH_3NH_3PbI_3$ and $CH_3NH_3PbBr_3$ form solid solutions while formation of solid solution is hindered for the combination of $CH_3NH_3PbI_3$ and $CH_3NH_3PbCl_3$ [4]. We have investigated fabrication of heterostructures using $CH_3NH_3PbI_3$ and $CH_3NH_3PbCl_3$ using vacuum deposition technique. In this paper, we report the first successful formation of $CH_3NH_3PbCl_3/CH_3NH_3PbI_3$ heterostructures.

2. Experimental

We sequentially deposited $CH_3NH_3PbI_3$ and $CH_3NH_3PbCl_3$ for single-heterostructure fabrication, and $CH_3NH_3PbCl_3$, $CH_3NH_3PbI_3$ and $CH_3NH_3PbCl_3$ for double-heterostructure formation on glass substrates using vacuum co-evaporation technique. The fluxes of supplied materials were kept constant by tuning materials temperatures with PID feedback. We set the rates of PbI_2 and $PbCl_2$ to 0.15 Å/s and total pressures of CH_3NH_3I and CH_3NH_3Cl to 0.007 Pa, respectively. The substrate temperature was kept at 21°C using cooled water.

Figure 1 shows XRD pattern ($2\theta/\omega$ scan) of a $CH_3NH_3PbI_3/CH_3NH_3PbCl_3$ (single-heterostructure) sample. We have confirmed that the sample does not change into single layer of homogenous alloy and that two independent I-

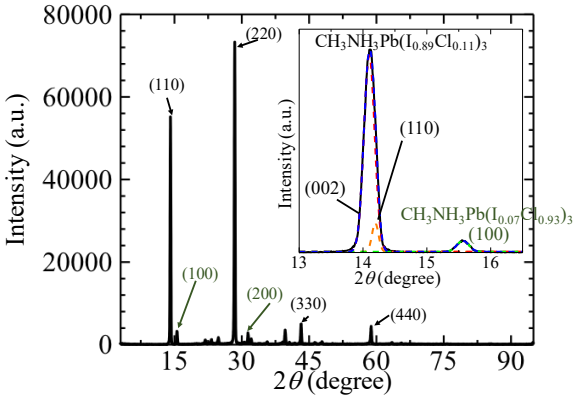

Fig. 1 XRD pattern ($2\theta/\omega$ scan) of $CH_3NH_3PbCl_3/CH_3NH_3PbI_3$/glass (single-heterostructure). The pattern around 15° is expanded in the inset.

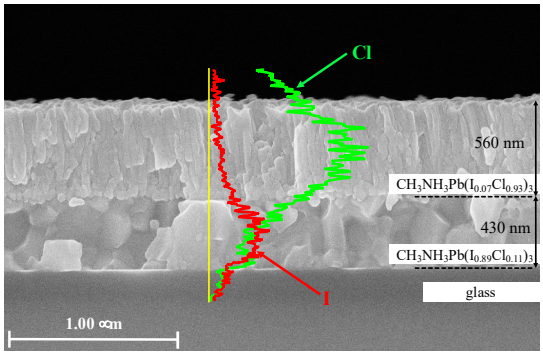

Fig. 2 SEM image of the fabricated single-heterostructure. The line distributions of I and Cl atoms on the yellow line are represented in red and green curves, respectively.

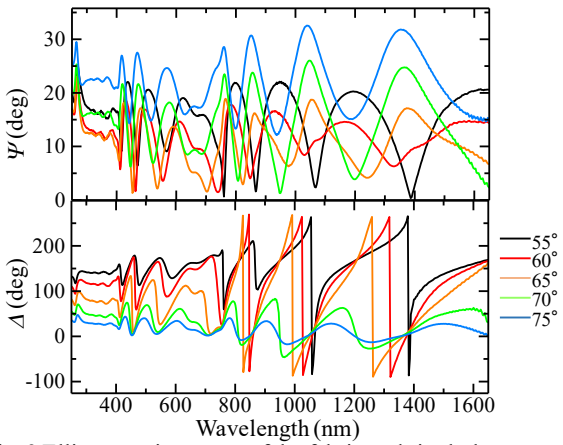

Fig. 3 Ellipsometric spectra of the fabricated single-heterostructure sample.

rich and Cl-rich $CH_3NH_3Pb(I_{1-x}Cl_x)_3$ phases exist. Concentrations of each phase estimated by assuming Vegard's law are $CH_3NH_3Pb(I_{0.89}Cl_{0.11})_3$ and $CH_3NH_3Pb(I_{0.07}Cl_{0.93})_3$. In cross-sectional SEM image of the single-hetero structure shown in Fig. 2(a), two separate layers (a 560-nm-thick $CH_3NH_3Pb(I_{0.07}Cl_{0.93})_3$ top layer with 40-nm-size grains and a 430-nm-thick $CH_3NH_3Pb(I_{0.89}Cl_{0.11})_3$ bottom layer with 100 nm-size grains) are clearly observed. Line distributions of chloride and iodide atoms shown in Fig. 2(a) also indicate successful formation of the heterostructure. Figure 3(a) represents ellipsometric spectra of the fabricated single-hetero structure sample. In the wavelength range from 400 nm (absorption edge of $CH_3NH_3Pb(I_{0.07}Cl_{0.93})_3$) and 750 nm (absorption edge of $CH_3NH_3Pb(I_{0.89}Cl_{0.11})$, interference fringes due to multiple reflections in the 560-nm-thick $CH_3NH_3Pb(I_{0.07}Cl_{0.93})_3$ top layer are clearly observed. Interference fringes observed in the wavelength range from 750 to 1600 nm are due to multiple reflections in the 1-μm-thick whole perovskite layers . The clear interference indicates that interface between two perovskite layers is satisfactorily abrupt, smooth and flat.

Figure 4(a) represents XRD pattern of a fabricated $CH_3NH_3PbCl_3/CH_3NH_3PbI_3/CH_3NH_3PbCl_3$ (double-heterostructure) sample. Two independent phases of $CH_3NH_3Pb(I_{0.96}Cl_{0.04})_3$ and $CH_3NH_3Pb(I_{0.01}Cl_{0.99})_3$ alloys are distinguished. As shown in cross-sectional SEM image (Fig. 4(b)), the double-heterostructure is successfully formed. The structure consists of a 220-nm-thick $CH_3NH_3Pb(I_{0.07}Cl_{0.93})_3$ top layer/a 710-nm-thick $CH_3NH_3Pb(I_{0.89}Cl_{0.11})_3$ intermediate layer/ a 650-nm-thick $CH_3NH_3Pb(I_{0.07}Cl_{0.93})_3$ bottom layer. Line profiles of iodide and chloride atoms also support successful formation of double-heterostructure. In ellipsometric spectra of the fabricated double-heterostructure sample shown in Fig. 5, observed interference fringes owing to multiple reflections are consistent with the sample structure.

We have confirmed that $CH_3NH_3PbBr_3/CH_3NH_3PbI_3$ sequential deposition leads to spontaneous alloying and thus heterostructure cannot be formed. Although slight alloying occurs in the $CH_3NH_3PbCl_3/CH_3NH_3PbI_3$ system, heterostructures can be fabricated as described above. We suggest that reduced spontaneous alloying in the $CH_3NH_3PbCl_3/CH_3NH_3PbI_3$ system can be attributed to the large difference between ion radii of chloride and iodide ions which hinders diffusion of iodide ions through chloride vacancies. This is supported by the fact that measured composition of iodide ions entering into $CH_3NH_3PbCl_3$ is smaller than that of chloride ions in $CH_3NH_3PbI_3$.

3. Conclusion

We have succeeded in fabricating single- and double-heterostructures based on the combination of $CH_3NH_3PbCl_3$ and $CH_3NH_3PbI_3$ by using sequential vacuum co-evaporation. Although spontaneous alloying slightly occurred, independent perovskite phases and layers were formed. The interfaces between perovskite semiconductors are optically flat, smooth and abrupt. The formation of the heterostructure is presumably owing to reduced interdiffusion of halide ions.

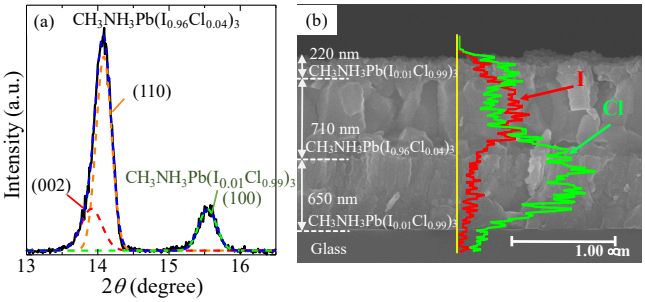

Fig. 4 XRD pattern ($2\theta/\omega$ scan) around 15° (a) and cross-sectional SEM image (b) of the fabricated double-heterostructure sample. The line distributions of I and Cl atoms on the yellow line are shown in red and green curves, respectively.

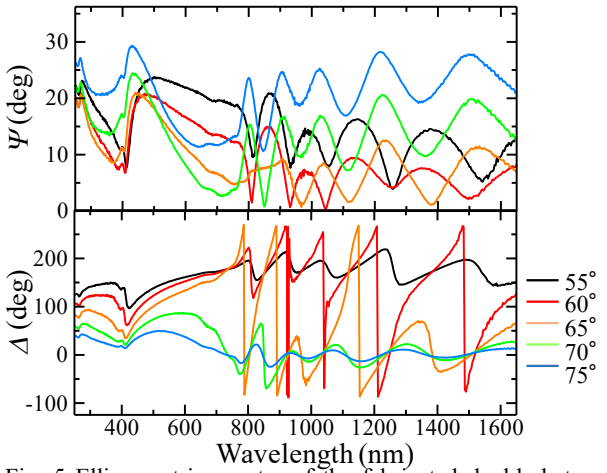

Fig. 5 Ellipsometric spectra of the fabricated double-heterostructure sample.

Acknowledgements

This work was partially supported by the NEDO project.

References

[1] U. Bansode and S. Ogale, J. Appl. Phys. **122** (2017) 133107.

[2] J. Sano, Y. Nakamura, T. Matsushita, and T. Kondo, Extended Abstract of the 76th JSAP meeting (2015) 14p-1G-6.

[3] C. Eames, J.M. Frost, P.R.F. Barnes, B.C. O'Regan, A. Walsh, and S. Islam, Nat. Commun. **6** (2015) 7497.

[4] N. Pellet, J. Teuscher, J. Malier, and M. Grätzel, Chem. Mater. **27,** (2015) 2181.